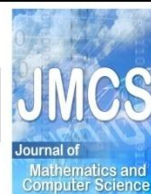Contents list available at JMCS

# Journal of Mathematics and Computer Science

Journal Homepage: www.tjmcs.com

# Investigation of the Coal Diameter Effect on Pulverized Coal Combustion for Pollutant Reduction

M.R. Safaie*

*Young Researchers and Elite Club, Mashhad Branch, Islamic Azad University, Mashhad, Iran* *Corresponding Author's* E-mail: cfd_safaei@yahoo.cm

B. Rahmanian

*Mashhad Branch, Islamic Azad University, Mashhad, Iran*

M. Goodarzi

*Mashhad Branch, Islamic Azad University, Mashhad, Iran*

### Abstract

The effect of increase diameter of coal particles on pulverized coal combustion to produce pollutants such as $NO_x$, CO, $CO_2$  and C in a 2D combustion chamber have been studied in this research by finite volume method. The numerical method is a generalized finite rate formulation, known as the Magnussen model, which is based on the solution of species transport equation for reactants and product concentration. The diameter of the pulverized coal varied from 0.0001 m to 0.0004 m which enters by the rate of 0.1 kg/s from the center of furnace. Moreover, air was preheated by a high-temperature gas generator, and the preheated oxidizer temperature could achieve $1400°C$. The results show that by increasing the diameter of pulverized coal, the rate of formation of pollutants as well as $NO_x$ and the temperature of the flame decreased.

**Keywords:** Pulverized Coal Combustion; Pollutants Reduction; Magnussen Model; Turbulent Flow.

## 1. Introduction

Atmospheric pollution has become a worldwide concern. This concern led to the consideration of the effects of injection large amounts of any species on the ozone balance in the atmosphere. When discussing nitrogen oxide formation from nitrogen in atmospheric air, one refers specifically to the $NO_x$ formed in combustion systems in which the original fuel contain no nitrogen atoms chemically bonded to other chemical elements such as carbon or hydrogen. Pulverized coal combustion is one of the major sources to produce energy for applications such as train and power plants. It is also one of the pollutant sources. However, air pollution is a major problem which strongly relative to human life. [1-3].

Zhang et al. [4] investigated numerically properties of pulverized coal combustion in high temperature air/steam mixture. They proved that the addition of steam into oxidizer will suppress the formation of $NO_x$ and the coal injecting velocity also has impacts on $NO_x$ formation. Therseen [5] proved numerically and experimentally the devolatilisation of high volatile bituminous coal particles under a rapid heating conditions. They obtained acceptable results for flame's peak temperature. In one of the recent works, Rahmanian et al. [6] studied the $NO_x$ reduction in pulverized coal combustion to reduce pollutants by finite volume method. Their research indicated

that the $NO_x$ reduction in pulverized coal combustion is more owing to injection of $CO_2$ in comparison with steam, Argon or Helium. In the present study, the $NO_x$ reduction via pulverized coal combustion in a 2-D combustion chamber, by changing the size of pulverized coal is studied. Simulation was done in four different diameters of the pulverized coal, 0.01mm, 0.02mm, 0.03mm and 0.04 mm.

## 2. Physical and Mathematical Models

The geometry of the problem is shown in Fig. 1.  The coal combustion system considered in this research is a 12m by 1m two dimensional furnace. Only half of the domain width is modeled because of the symmetry. The inlet of the 2D furnace is split into two streams. A high-speed stream near the center of the furnace at 30 m/s and spans 0.125 m and the other stream enters at 10 m/s and spans 0.375 m. both streams are air at the temperature of 1400 k. The flow is considered turbulent, and it is assumed that pulverized coal combustion is steady [7-8]. The coal particles are also taken to be spherical.
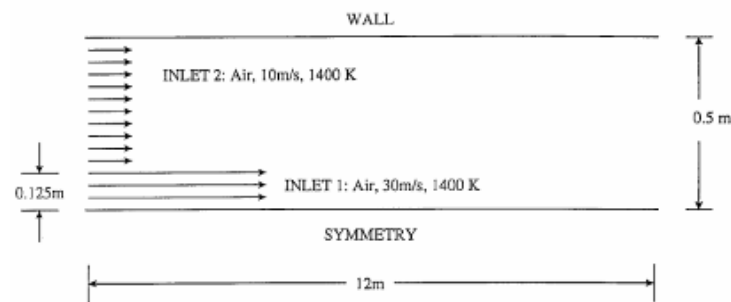


Figure 1. Schematic of the problem [6]

The government equations can be written as:

$$\frac{\partial U}{\partial x} + \frac{\partial V}{\partial y} = 0 \tag{1}$$

$$\frac{\partial U}{\partial t} + U\frac{\partial U}{\partial x} + V\frac{\partial U}{\partial y} = -\frac{\partial P}{\partial x} + \frac{1}{\text{Re}}(\frac{\partial^2 U}{\partial x^2} + \frac{\partial^2 U}{\partial y^2}) \tag{2}$$

$$\frac{\partial V}{\partial t} + U\frac{\partial V}{\partial x} + V\frac{\partial V}{\partial y} = -\frac{\partial P}{\partial y} + \frac{1}{\text{Re}}(\frac{\partial^2 V}{\partial x^2} + \frac{\partial^2 V}{\partial y^2}) + \frac{Ra}{\text{Pr}.\text{Re}^2}T \tag{3}$$

$$\frac{\partial T}{\partial t} + U\frac{\partial T}{\partial x} + V\frac{\partial T}{\partial y} = -\frac{\partial P}{\partial y} + \frac{1}{\text{Pr}.\text{Re}}(\frac{\partial^2 T}{\partial x^2} + \frac{\partial^2 T}{\partial y^2}) \tag{4}$$

$$\frac{\partial}{\partial t}(\rho Y_i) + \nabla.(\rho\vec{\upsilon}Y_i) = -\nabla.\vec{J} + R_i + S_i \tag{5}$$

where $R_i$ is the net production rate of species $i$ by chemical reaction, $S_i$ is the creation rate by addition from the dispersed phase plus any user-defined sources, and $Y_i$ shows the local mass fraction of each species via the solution of a convection-diffusion equation for the $i^{th}$ species. In turbulent flows, the mass fraction $J_i$ of equation (5) is shown in equation (6):

$$\vec{J_i} = -(\rho D_{i,m} + \frac{\mu_t}{Sc_t})\nabla Y_i \qquad (6)$$

where $Sc_t$ is the turbulent Schmidt number.

The net rate of species $i$ production due to reaction $r$, $R_{i,r}$ is given by the smaller of the two expressions as shown in equations (7) and (8).

$$R_{i,r} = \upsilon'_{i,r}M_{w,i}A\rho\frac{\varepsilon}{k}\min(\frac{Y_R}{\upsilon'_{R,r}M_{w,R}}) \qquad (7)$$

$$R_{i,r} = \upsilon'_{i,r}M_{w,i}AB\rho\frac{\varepsilon}{k}\frac{\sum_P Y_P}{\sum_J^N \upsilon''_{J,r}M_{w,j}} \qquad (8)$$

where $k/\varepsilon$ is the large eddy mixing time scale as in Spalding's eddy breakup model, $M_{w,i}$ is the molecular weight of species $i$, $\upsilon_{i,r}$ is the stoichiometric coefficient for reactant $i$ in reaction $r$, $Y_P$ is the mass fraction of any product species, P, $Y_R$ is the mass fraction of a particular reactant, and A, B are empirical constants equal to 4.0 and 0.5 respectively [7].

The RNG k-ε turbulent model [9] was used in the present study to account for turbulent effects.

Turbulent Kinetic Energy Transport (K) equation:

$$\frac{\partial(\rho k)}{\partial t} + \nabla\cdot(\rho\vec{u}k) = \nabla\cdot\left[\left(\mu + \frac{\mu_t}{\sigma_k}\right)\nabla k\right] + G_k - \rho\varepsilon + P_K \qquad (9)$$

Dissipation of Turbulent Kinetic Energy Transport $(\varepsilon)$ equation:

$$\frac{\partial(\rho\varepsilon)}{\partial t} + \nabla\cdot(\rho\vec{u}\varepsilon) = \nabla\cdot\left[\left(\mu + \frac{\mu_t}{\sigma_\varepsilon}\right)\nabla\varepsilon\right] + \frac{\varepsilon}{k}(C_1 P_K + C_2 + C_3 G_k) - R_\varepsilon \qquad (10)$$

where

$$R_\varepsilon = \frac{C_\mu\rho\eta^3\left(1 - \frac{\eta}{\eta_0}\right)}{1 + \beta\eta^3}\frac{\varepsilon^2}{k} \qquad (11)$$

and

$$\eta = \frac{Sk}{\varepsilon} \qquad (12)$$

Using the Prandtl- Kolmogorov relation, the eddy viscosity can be expressed as follows:

$$\upsilon_t = C_\mu f_\mu \frac{k^2}{\varepsilon} \qquad (13)$$

The turbulence energy production term, $P_k$, can be obtained by:

$$P_k = \upsilon_t\left[2\left(\frac{\partial u}{\partial x}\right)^2 + 2\left(\frac{\partial v}{\partial x}\right)^2 + \left(\frac{\partial u}{\partial y} + \frac{\partial v}{\partial y}\right)^2\right] \qquad (14)$$

The buoyancy term, $G_k$, is defined as:

145

$$G_k = -g\beta \frac{\upsilon_t}{\sigma_t} \frac{\partial T}{\partial y}$$

(15)

The model constants in the above equations are listed in Table 1.

Table 1. Coefficients for RNG k-ε turbulent model [9]

| $C_\mu$ | $\sigma_k$ | $\sigma_\varepsilon$ | $C_1$ | $C_2$ | $\eta_0$ | $\beta$ | K |
|---------|-----------|----------------------|-------|-------|----------|---------|-----|
| 0.0845  | 1         | 1.3                  | 1.42  | 1.68  | 4.38     | 0.012   | 0.41 |

Discrete Ordinates (DO) radiation model for spectral intensity is [10]:

$$\nabla \cdot (I_\lambda(\vec{r},\vec{s})\vec{s}) + (a_\lambda + \sigma_s)I_\lambda(\vec{r},\vec{s}) = a_\lambda n^2 I_{b\lambda} + \frac{\sigma_s}{4\pi} \int_0^{4\pi} I_\lambda(\vec{r},\vec{s}')\phi(\vec{s},\vec{s}')d\Omega'$$

(16)

The total intensity $(I(\vec{r},\vec{s}))$ in direction $\vec{s}$ at position $\vec{r}$ is calculated by:

$$I(\vec{r},\vec{s}) = \sum_k I_{\lambda_k}(\vec{r},\vec{s})\Delta\lambda_k$$

(17)

The two dimensional flow described by these equations is represented by the two velocity components U, V which, respectively, correspond to the two coordinate direction x, y.

## 3.  Numerical Procedure and Boundary Condition

In order to solve the differential equations that govern the flow, the finite volume method, which is explained in details by Patankar [11] and Safaei et al. [12-13], was used. This method is a specific case of residual weighting method. In this approach, the computational field is divided to some control volumes in a way that a control volume surrounds each node and control volumes have no volumes in common. Then, the differential equation is integrated on each control volume. Profiles in pieces that show changes (of a certain quantity like temperature, velocity, etc.) among the nodes are used to calculate the integrals. The result is discretization equation, which includes quantities for a group of nodes [11-13]. The advantage of this method is high accuracy even in low nodes. Quick scheme was adopted for the discretization of all convective terms of the advective transport equations. The final discretized forms of the equations were solved by using the SIMPLE algorithm [14-16]. The coal combustor studied in this research is a non-adiabatic system. The generalized finite rate chemistry model, mentioned as the Magnussen model, was employed due to the flow in the mixture with turbulence. In this flow, four boundary conditions exist. The first boundary condition is the velocity inlet, which is used to define flow velocity along with all relevant scalar flow properties at the flow inlets. The second is the wall condition, which is used to bound fluid regions. The next boundary condition is the pressure outlet condition, used in all kinds of flow fields such as laminar and turbulent flow. The last boundary is the axis condition. The axis boundary type must be used as the centerline of an axisymmetric geometry.

## 4.  Validation

For proving the validation of the present work, the problem defined by Rahmanian and Ghazikhani [17] has been analyzed, solved and compared with the present work. The comparison between the present work and Rahmanian and Ghazikhani`s [17] result are illustrated in Figs. 2 (a and b).  As

can be seen, there is a reasonable agreement between the results of Rahmanian and Ghazikhani [17] study and the results of present work.
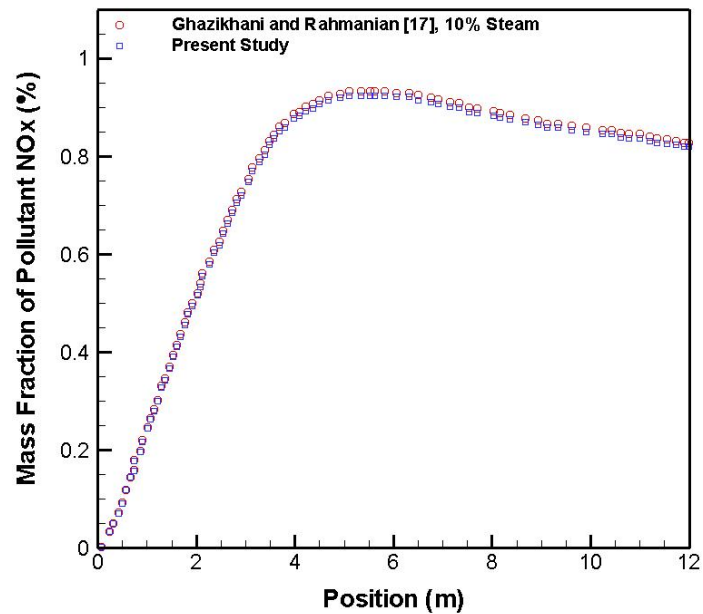


a) Mass fraction of $NO_x$
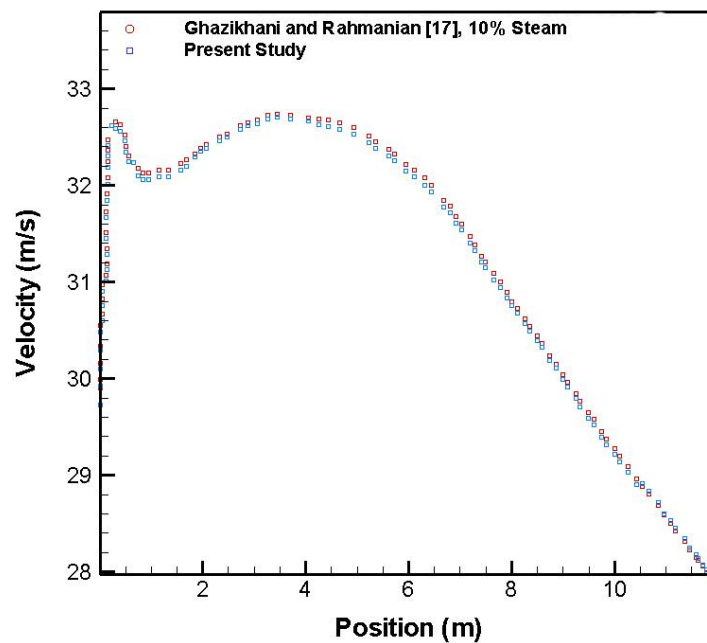


b) Axial velocity distribution

Figure 2. Comparison of the predicted mass fraction of pollutant $NO_x$ and axial velocity distribution along the centerline of the burner with the experimental data of Ghazikhani and Rahmanian [17]

## 4.1 Grid Independence

The computational domain was discretized via structured, non-uniform grid distributions. The grid seems more refined in the vicinity of walls with significant temperature and velocity gradients.

Several grid distributions were tested to assure that the computational results are grid-independent. Fig. 3 illustrates the result of the grid independence studies. Based on the outcome, a grid distribution 1200×50 was selected for all the modeling cases.
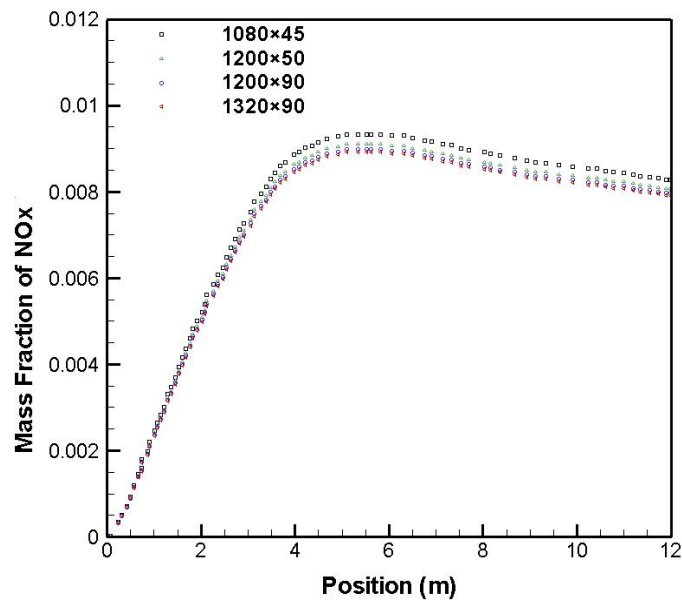


Figure 3. Grid independence tests for the present study by comparison mass fraction of $NO_x$ in various mesh concentration

## 5.   Results and Discussion

The results of pulverized coal combustion modeling illustrated under influence of varied diameter of pulverized coal. All plots are according to centerline of the furnace.
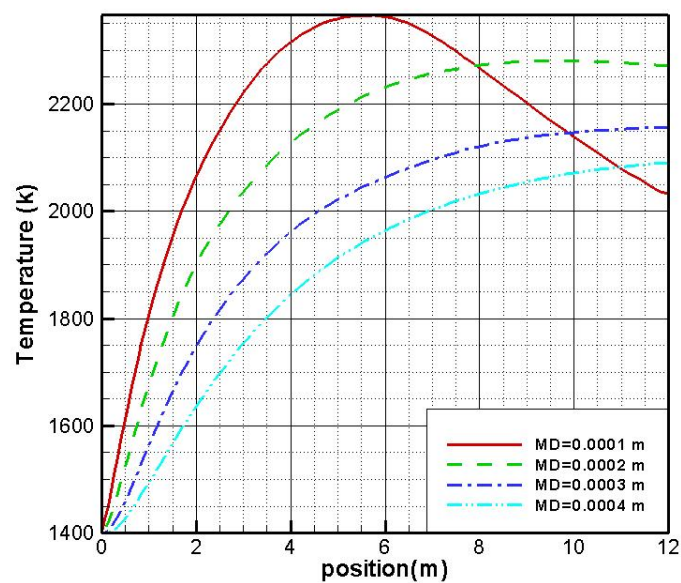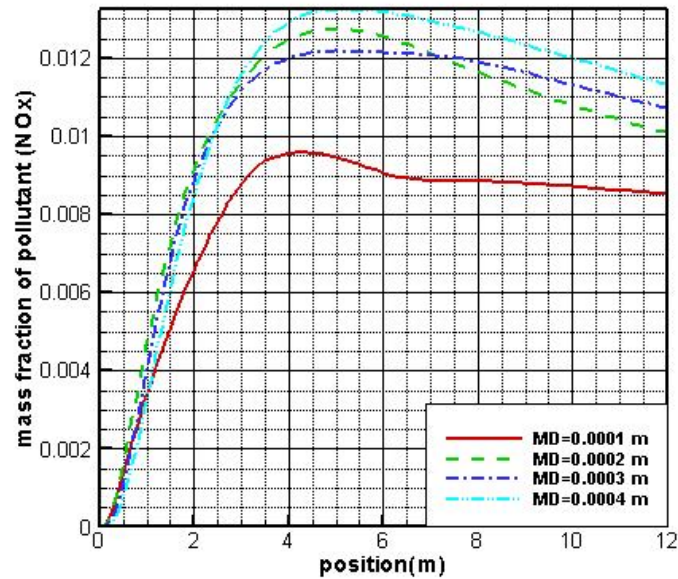


Figure 4. Temperature Profiles

Figure 5. Mass Fraction of $NO_x$ Profiles

Figs. 4 and 5 shows that the temperature of the flame will decrease due to increase of diameter of pulverized coal but some pollutants such as $NO_x$ increased. For non-premixed systems like pulverized coal combustion and almost obtained in carbureted spark ignition engines, the temperature, and hence the mixture ratio, is the prime parameter in determining the quantities of NOx formed.
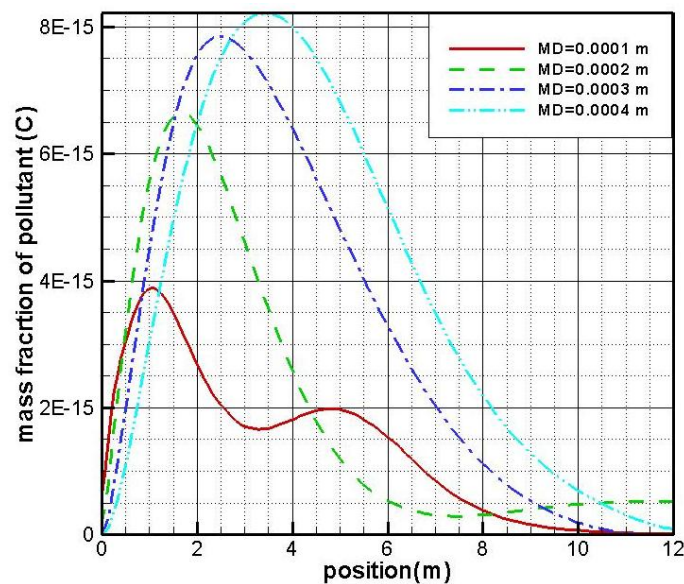


Figure 6. Mass Fraction of C Profiles

According to fig. 6, the rate of mass fraction of C will be suppressed as a result of size of pulverized coal molecule. The main reason for this phenomenon is increasing of mean diameter of pulverized coal, which restricts the $NO_x$ formation by thermal $NO_x$ mechanism.
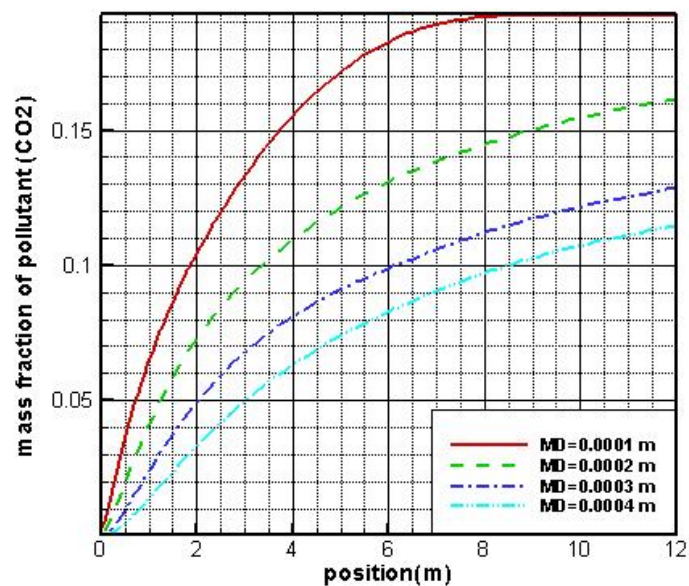
Figure 7. Mass Fraction of $CO_2$ Profiles

Fig. 7 illustrated the mass fraction of $CO_2$ at the center of furnace. As can be seen from the diagram, increasing the diameter of pulverized coal causes an impressive reduction in producing pollutants. In the case of present study, decreasing the size of coal particles form 0.04 mm to 0.01 mm, increase the $CO_2$ pollutant more than 65%.
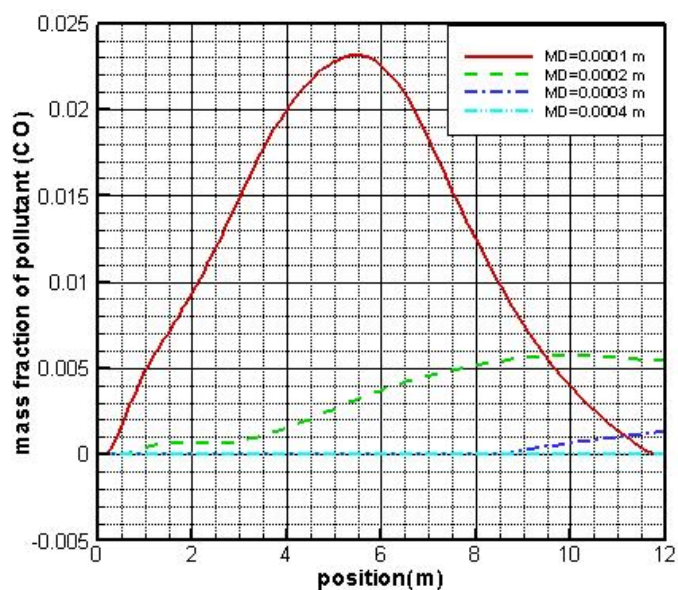


Figure 8. Mass Fraction of CO Profiles

The mass fraction of CO pollutant in the center of furnace is being represented via Fig. 8. With a short glance, it is obvious that increasing the diameter of coal particles can reduce the CO pollutant severely. Especially in MD=0.04mm, there is almost no CO pollutant in the exhaust gases.

## 6. Conclusion

In this research, effect of increase the diameter of coal particles on pulverized coal combustion to produce pollutants such as $NO_x$, CO, $CO_2$ and C in a 2D combustion chamber have been studied.

A numerical method which incorporates pressure based algorithm and implicit solver has been employed to simulate non-premix combustion model. As can be seen from above diagrams, increase the diameter of pulverized coal causes the temperature of the flame and the pollutants formation rate -except $NO_x$ formation rate- greatly decrease.

## Acknowledgment

## References

[1]   J. Kagawa, Health effects of diesel exhaust emissions—a mixture of air pollutants of worldwide concern, Toxicology, Vols. 181–182 (2002) 349–353.

[2]   Japan Auto. Res. Ins., Report for automobile emission and chronic obstructive lung disease in small animals (Ch. Res. Act. Comm.: J. Kagawa). Japan Auto. Res. Ins., Tsukuba, Japan, 1994.

[3]   Japan Env. Agen., Dep. Env. Heal., A study report of the research method of health effects of local air pollution by animal exposure experiment (Ch. Res. Act. Comm.: J. Kagawa), Japan Env. Agen., Japan, 1999.

[4]   Q. Zhang, A. Swiderski, W. Yang and B. Wlodzimierz, Properties of pulverized coal combustion in high temperature air/steam mixture, Roy. Ins. of tech., 2006.

[5]   E. Therssen, L. Gourichon and L. Delfosse, Devolatilization of coal particles in a flat flame, Comb. Flame, Vol. 103, pp.115-128, 1995.

[6]   Behnam Rahmanian, Mohammad Reza Safaei, Salim Newaz Kazi, Goodarz Ahmadi, Hakan Fehmi Oztop, Kambiz Vafai, Investigation of pollutant reduction by simulation of turbulent non-premixed pulverized coal combustion, App. Therm. Eng. (2014) Accepted for publish.

[7]   Norbert Peters, Turbulent Combustion, Cambridge University Press, 2000.

[8]   Thierry Poinsot and Denis Veynante, Theoretical and Numerical Combustion, R. T. Edwards, Inc., 2005.

[9]   M. Goodarzi, M.R. Safaei, K. Vafai, G. Ahmadi, M. Dahari, S. Kazi and N. Jomhari, Investigation of nanofluid mixed convection in a shallow cavity using a two-phase mixture model, Int. J. Therm. Sci., 75 (2014) 204-220.

[10]  M. Goodarzi, M.R. Safaei, Hakan F. Oztop, E. Sadeghinezhad, M. Dahari and S.N. Kazi, Numerical Study of Entropy Generation due to Coupled Laminar and Turbulent Mixed Convection and Thermal Radiation in an Enclosure Filled with a Semitransparent Medium, Sci. World J., vol. 2014, Article ID 761745, 8 pages, (2014) doi:10.1155/2014/761745.

[11]  S. V. Patankar, Numerical heat transfer and fluid flow, Washigton DC: Hemisphere publishing corporation, 1980.

[12]  M. R. Safaei, B. Rahmanian and M. Goodarzi, Numerical study of laminar mixed convection heat transfer of power-law non-Newtonian fluids in square enclosures by finite volume method, Int. J. Phys. Sci., Vol. 6(33) (2011) 7456 – 7470.

[13]  M. R. Safaei, H. R. Goshayeshi, B. Saeedi Razavi and M. Goodarzi, Numerical investigation of laminar and turbulent mixed convection in a shallow water-filled enclosure by various turbulence methods, Sci. Res. Essays, 6(22), (2011) 4826-4838.

[14]  M. R. Safaei, M. Goodarzi and M. Mohammadi, Numerical modeling of turbulence mixed convection heat transfer in air filled enclosures by finite volume method, Int. J. Multiphysics, 5 (2011).

[15]  A. Karimipour, M. Afrand, M. Akbari and M. R. Safaei, Simulation of Fluid Flow and Heat Transfer in the inclined enclosure, Int. J. Mech. Aerospace Eng., 6 (2012), 86-91, 2012.

[16]  M. R. Safaei, B. Rahmanian and M. Goodarzi, Numerical Study of Laminar Mixed Convection Heat Transfer of Power-Law Non-Newtonian Fluids in Square Enclosures by Finite Volume Method, Int. J. Phys. Sci., 6(33), 7456 - 7470, 2011.

[17]  B. Rahmanian, M. Ghazikhani, Effect of steam injection in pulverized coal combustion to reduce pollutants, 6th Int. Chem. Eng. Cong. (2009) Kish Island, Iran.